

## Coffee Husk as Corrosion Inhibitor for Mild Steel in HCl Media

Renata F. B. Cordeiro<sup>1,\*</sup>, Allan J. S. Belati<sup>1</sup>, Daniel Perrone<sup>2</sup>, Eliane D'Elia<sup>1</sup>

<sup>1</sup> Department of Inorganic Chemistry, Chemistry Institute, Federal University of Rio de Janeiro, Brazil

<sup>2</sup> Laboratory of Nutritional Biochemistry and Food, Department of Biochemistry, Chemistry Institute, Federal University of Rio de Janeiro, Brazil

\*E-mail: [rbcordeiro@gmail.com](mailto:rbcordeiro@gmail.com)

Received: 7 August 2018 / Accepted: 19 September 2018 / Published: 5 November 2018

---

The corrosion inhibition of mild steel by coffee husk aqueous extract (1) and its high molecular weight fraction (2) was investigated in 1 mol L<sup>-1</sup> HCl medium. Gravimetric tests showed that for both inhibitors, inhibition efficiency (*IE*) increased with time and extract concentration, reaching a *IE* of 89.2% and 90.3% for 800 mg L<sup>-1</sup> of inhibitors (1) and (2), respectively, in 24 h of immersion. Gravimetric tests varying temperature showed the activation energy (*E<sub>a</sub>*) barely varied for Inhibitor 1. For Inhibitor 2 a decrease in *E<sub>a</sub>* was noted, a hint it is attached on the metal surface by chemisorption. Polarization curves indicated that both extracts act as mixed type inhibitors. Impedance results showed a decrease in double layer capacitance (*C<sub>dl</sub>*) and an increase in charge transfer resistance (*R<sub>ct</sub>*), with a better performance for inhibitor (2). Both extracts presented a good linearity with respect to Langmuir isotherm, an evidence of a monolayer formation. Our results suggest inhibitor 1 acts by purely blocking the metal surface, and in case of inhibitor 2, it screens the metal surface and reduces the activation energy.

---

**Keywords:** Mild steel, corrosion inhibitor, coffee husk, waste, natural products.

### 1. INTRODUCTION

The use of corrosion inhibitors is one of the most effective ways of stopping/retarding corrosion, which is why industries apply them to protect equipment, industrial plants, and refrigeration systems in the production, transport, and storage of oil and natural gas [1-4]. Increased environmental awareness coupled with the high cost of synthetic inhibitors boosted research for environmentally friendly inhibitors from various parts of plants including seeds, leaves, stems, fruits and peels, as well as the bagasse, and these studies have achieved great results by groups all over the globe [5 – 13], including ours [14 – 20].

Among the natural sources of inhibitory substances, coffee and its various parts have been studied [21 – 26]. Each year, more than 500 million cups of coffee are consumed, making it one of the

most popular drinks in the world [27]. Approximately 40% of coffee weight is made of husk, and currently, this residue does not have a very noble destination, being used as furnace fuel or feed enrichment for cattle [21, 28]. Our research group has been conducting studies on coffee residues, such as coffee grounds, as a corrosion inhibitor for 1020 mild steel in acidic medium and achieved interesting results with coffee grounds extract [29]: a maximum inhibition efficiency of 97% was obtained in 24 hours of immersion, in the presence of 400 mg L<sup>-1</sup> of the extract obtained by decoction.

We also hypothesized [30] that the inhibitory action of the roasted coffee extract can be explained by the presence of melanoidins, which are compounds formed during coffee roasting [31]. These molecules form a heterogeneous class, whose structure is complex, derived from polysaccharides and proteins, but still remain fairly unknown [32]. The melanoidins formed during the roasting of coffee make up a large part of the beverage, reaching up to 25% of the dry matter [33].

The aim of this work was to study the extract from coffee husks and its high molecular weight fraction as a corrosion inhibitor for mild steel 1020 in HCl medium. We also look forward to understand how the extracts work on the metal surface to protect it against corrosion.

## 2. METHODS

### 2.1. Material and medium

The mild steel coupons used for all the experiments had the following composition (% by weight): C: 0.18, P: 0.04, S: 0.05, Mn: 0.30, Si: trace and Fe: balance. For gravimetric assays the coupons were abraded with 100 mesh water grit paper, sandblasted, washed with doubly distilled water, degreased with acetone and hot air dried. For electrochemical assays coupons were abraded using the AROPOL 2V (AROTEC) polishing machine and water grit paper having a granulometry of 100, 320, 600, 1200 and 2000 mesh, washed with doubly distilled water, degreased with acetone and hot air dried.

The corrosive solution, 1 mol L<sup>-1</sup> HCl, was prepared from 37% HCl (Merck Co. -Darmstadt - Germany) and doubly distilled water. The concentration range of the extract used was 50–1000 mg L<sup>-1</sup> and the volume of the electrolyte used was 100 mL in each experiment.

### 2.2. Obtaining the extract

#### 2.2.1. Aqueous coffee husk extract (Inhibitor 1)

Coffee husks from *Coffea Arabica* species were initially ground. 10.0 g of coffee husks were placed in 100 mL of double distilled boiling water for 1 hour infusion. Filtration was then performed in cotton filters and the filtrate was stored in glass containers and placed in a freezer at -4 °C.

The containers with the frozen filtrate were lyophilized (Liotop; model L101) at an average temperature of -52 °C, generating a powder as final product.

### 2.2.2. High molecular weight fraction (HMWF) (Inhibitor 2)

The HMWF was isolated from the aqueous coffee husks extract (Inhibitor 1) by diafiltration. Briefly, aqueous coffee husks extract was poured in a ultrafiltration 3 kDa cut-off membrane (Millipore) and submitted to centrifugation at 3500 rpm. The HMWF retained by the membrane was then washed with double distilled water, again through centrifugation. This process was repeated until the washing eluate was colorless. The final retentate was frozen and lyophilized.

### 2.3. Gravimetric and electrochemical measurements

The gravimetric and electrochemical measurements have been detailed in our previous works [14,16].

Weight loss were performed varying time from 2 to 48 h, inhibitor concentration from 50 to 1000 mg L<sup>-1</sup> and temperature from 25 to 55 °C. Each assay was made in triplicate; the inhibition efficiency (*IE*%) was obtained by the average from these replicated values and it was calculated from equation 1 [29]:

$$IE\% = [(W_{corr,0} - W_{corr}) / W_{corr,0}] \times 100 \quad (1)$$

Where  $W_{corr,0}$  and  $W_{corr}$  are the corrosion rates in the absence and presence of the extract, respectively, in g cm<sup>-2</sup> h<sup>-1</sup>.

The data obtained with the tests varying temperature was used to build an Arrhenius plot, based on equation 2

$$\ln W_{corr} = \ln A - (E_a/RT) \quad (2)$$

Where  $A$  is the frequency factor,  $E_a$  is the apparent activation energy,  $R$  is the constant for ideal gases and  $T$  is the absolute temperature.

All electrochemical measurements were executed on a typical three-electrode Pyrex cell. The working electrode was a mild steel coupon, the reference electrode was a saturated calomel electrode and the counter electrode was a platinum wire with large area. The tests were performed in a model AUTOLAB – PGSTAT 128 N potentiostat/galvanostat with a Metrohm impedance module.

Before the electrochemical measurements, the OCP was monitored for 4000 s, the necessary amount of time to achieve its stabilization. Impedance measurements were executed by applying 10 mV (rms) as a disturbance in a frequency band ranging from 100 kHz to 10 mHz, with polarized working electrode at the open circuit potential.  $R_{ct}$  was used in equations 3 and 4 to calculate the degree of surface coverage ( $\theta$ ) and the inhibition efficiency, *IE*%.

$$IE\% = [(R_{ct} - R_{ct,0}) / R_{ct}] \times 100 \quad (3)$$

$$\theta = (R_{ct} - R_{ct,0}) / R_{ct} \quad (4)$$

Where  $R_{ct,0}$  and  $R_{ct}$  are the mild steel charge transfer resistances in 1 mol L<sup>-1</sup> HCl medium in the absence and presence of the inhibitor, respectively.

Polarization curves were acquired varying the potential from -300 mV to +300 mV with respect to the OCP at 1 mV s<sup>-1</sup> scan rate. The inhibition efficiencies, *IE*%, were calculated from equation 5 [29]:

$$IE\% = [(j_{corr,0} - j_{corr}) / j_{corr,0}] \times 100 \quad (5)$$

Where  $j_{corr,0}$  and  $j_{corr}$  are the corrosion current densities of mild steel in 1 mol L<sup>-1</sup> HCl medium in the absence and presence of the inhibitor, respectively.

#### 2.4. Surface characterization by Scanning Electron Microscopy (SEM)

The morphologies of the uninhibited and inhibited mild steel surfaces were analyzed by SEM. Coupons were mechanically abraded with water grit paper of 100 to 2000 mesh granulometry, after abrasion the samples were washed with doubly distilled water, degreased with acetone and dried. Each coupon was immersed in the acid solution for 2 hours, in the absence and presence of 200 mg L<sup>-1</sup> of each inhibitor; after the elapsed time they were removed from the solution, washed with doubly distilled water, degreased with acetone and dried. They were analyzed on a scanning electron microscope, JEOL JSM 6460LV with an acceleration voltage of 20 kV. The images were increased 1000x.

#### 2.5. Spectroscopic characterization by nuclear magnetic resonance (NMR)

Inhibitors 1 and 2 were characterized by one-dimensional <sup>1</sup>H NMR spectroscopy. The spectra were measured at 500 MHz on a Bruker AVIII 500 spectrometer equipped with a 5 mm z-gradient SmartProbe. Spectra were obtained at 300 K and DSS (sodium salt of 2,2-dimethyl-2-silapentane-5-sulphonic acid) was used as an internal reference calibrated to 0 ppm. The water signal was suppressed by presaturation at 4.7 ppm with the acquisition parameters as follows: 32k data points, 7 kHz spectral width, 2.4 s acquisition time, 3.0 s relaxation delay time and 128 number of scans.

### 3. RESULTS AND DISCUSSION

#### 3.1. Study of the aqueous coffee husk extract – Inhibitor 1

##### 3.1.1 Gravimetric measurements

Table 1 shows the results for tests varying extract concentration and time for inhibitor 1.  $W_{corr}$  decreased, and consequently  $IE$  increased, as the concentration increased for all the tested times. We can assume that higher concentrations help in the formation of a protective layer over the metal surface.  $W_{corr}$  also decreased with increasing time, indicating the adsorption of the coffee husks extract components on the mild steel was relatively long. Higher  $IE$  values with longer immersion time also showed the stability of the inhibitor film on the metal surface. The extract acts as a corrosion inhibitor, weakening the attack by the corrosive media.  $IE$  did not significantly vary after 24h, likely due to a saturation of the metal surface with inhibitor molecules [8, 34].

**Table 1.** Results of the gravimetric assays for mild steel varying time and concentration of inhibitor 1.

Immersion time (h)	Inhibitor (mg L <sup>-1</sup> )	$W_{corr}$ (g cm <sup>-2</sup> h <sup>-1</sup> )	Standard deviation (g cm <sup>-2</sup> h <sup>-1</sup> )	$IE$ (%)
2	0	$2.80 \times 10^{-3}$	$5 \times 10^{-5}$	-
	100	$1.67 \times 10^{-3}$	$5 \times 10^{-5}$	40.4
	200	$1.60 \times 10^{-3}$	$2 \times 10^{-5}$	42.9
	400	$1.36 \times 10^{-3}$	$4 \times 10^{-5}$	51.6
	800	$1.11 \times 10^{-3}$	$8 \times 10^{-5}$	60.2
	1000	$1.20 \times 10^{-3}$	$2 \times 10^{-5}$	57.1
4	0	$1.91 \times 10^{-3}$	$4 \times 10^{-5}$	-
	100	$1.08 \times 10^{-3}$	$<1 \times 10^{-5}$	43.3
	200	$8.96 \times 10^{-4}$	$6 \times 10^{-6}$	53.1
	400	$7.55 \times 10^{-4}$	$2 \times 10^{-6}$	60.5
	800	$6.29 \times 10^{-4}$	$2 \times 10^{-5}$	67.1
	1000	$5.61 \times 10^{-4}$	$3 \times 10^{-5}$	70.6
24	0	$1.65 \times 10^{-3}$	$<1 \times 10^{-5}$	-
	100	$7.31 \times 10^{-4}$	$2 \times 10^{-5}$	55.8
	200	$5.61 \times 10^{-4}$	$3 \times 10^{-6}$	66.1
	400	$2.42 \times 10^{-4}$	$6 \times 10^{-6}$	85.3
	800	$1.79 \times 10^{-4}$	$2 \times 10^{-5}$	89.2
	1000	$1.61 \times 10^{-4}$	$7 \times 10^{-6}$	90.3
48	0	$1.86 \times 10^{-3}$	$<1 \times 10^{-5}$	-
	100	$9.09 \times 10^{-4}$	$<1 \times 10^{-6}$	51.0
	200	$6.84 \times 10^{-4}$	$4 \times 10^{-5}$	63.1
	400	$5.60 \times 10^{-4}$	$5 \times 10^{-6}$	69.8
	800	$1.35 \times 10^{-4}$	$5 \times 10^{-6}$	92.7
	1000	$1.14 \times 10^{-4}$	$<1 \times 10^{-6}$	93.9

The effect of the temperature on the corrosion of mild steel in acid solution was evaluated in the presence of 200 mg L<sup>-1</sup> of inhibitor 1, between 25 °C and 55 °C, with an immersion time of 2 hours, as shown in Table 2.

**Table 2.** Results of the gravimetric tests in the presence and absence of 200 mg L<sup>-1</sup> of inhibitor 1 for 2 hours varying temperature.

Temperature (°C)	Blank		Inhibitor 1		IE (%)
	$W_{corr}$ (g cm <sup>-2</sup> h <sup>-1</sup> )	Standard deviation (g cm <sup>-2</sup> h <sup>-1</sup> )	$W_{corr}$ (g cm <sup>-2</sup> h <sup>-1</sup> )	Standard deviation (g cm <sup>-2</sup> h <sup>-1</sup> )	
25	3.00 x 10 <sup>-3</sup>	1 x 10 <sup>-4</sup>	1.66 x 10 <sup>-3</sup>	7 x 10 <sup>-5</sup>	44.6
35	4.62 x 10 <sup>-3</sup>	<1 x 10 <sup>-5</sup>	2.51 x 10 <sup>-3</sup>	5 x 10 <sup>-5</sup>	45.6
45	8.62 x 10 <sup>-3</sup>	5 x 10 <sup>-5</sup>	5.26 x 10 <sup>-3</sup>	2 x 10 <sup>-4</sup>	39.0
55	1.21 x 10 <sup>-2</sup>	<1 x 10 <sup>-4</sup>	6.96 x 10 <sup>-3</sup>	4 x 10 <sup>-5</sup>	42.4

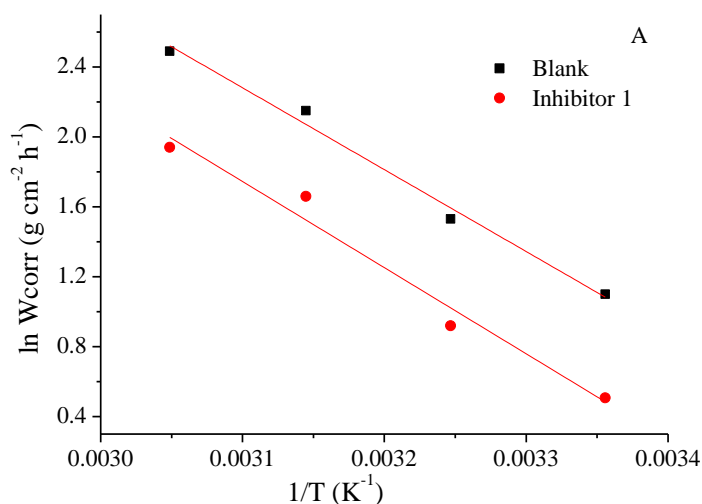
Corrosion rates increased with the temperature for the blank assays and for the assays containing the extract in the same magnitude. These results indicate that there was no significant change in the inhibition efficiency for inhibitor 1 as the temperature increased.

The Arrhenius plot (Fig. 1 A) shows parallel curves, suggesting that the apparent activation energy remains constant in the presence of inhibitor 1.

We used an alternative form of the Arrhenius equation (6) to calculate the entropy and enthalpy of activation [35]:

$$W_{corr} = RT/Nh \exp(\Delta S^*/R) \exp(-\Delta H^*/RT) \tag{6}$$

Where N is the Avogadro number, h is the Planck constant,  $\Delta S^*$  is the entropy of activation and  $\Delta H^*$  is the enthalpy of activation. A plot of  $\ln(W_{corr}/T)$  vs.  $1/T$  yields a line with a slope of  $-\Delta H^*/R$  and an intercept of  $\ln(R/Nh) + \Delta S^*/R$  (Fig. 1 B).



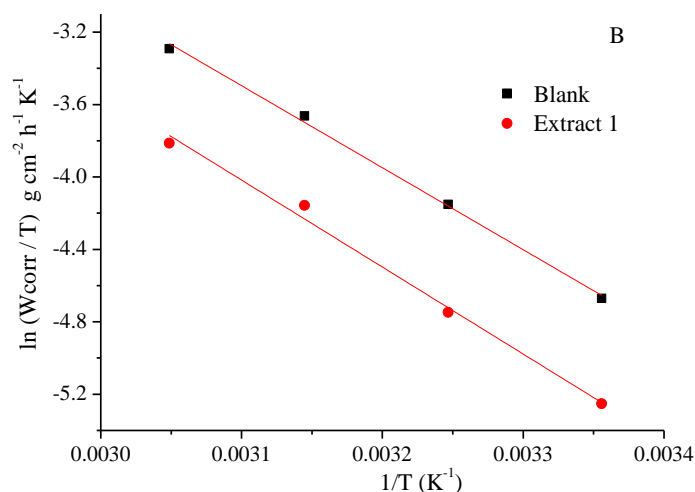


**Figure 1.** Arrhenius plot (A)  $\ln W_{\text{corr}} \times 1/T$  and (B)  $\ln(W_{\text{corr}}/T) \times 1/T$  for mild steel in  $1 \text{ mol L}^{-1}$  in the absence and presence of inhibitor 1.

Comparing the values obtained for the blank assays with the values for inhibitor 1, the numbers do not significantly differ. The activation energy was  $40.2 \text{ kJ mol}^{-1}$  in the absence and  $42.5 \text{ kJ mol}^{-1}$  in the presence of inhibitor 1, a hint for the mechanism of inhibition, showing Inhibitor 1 is of a pure blocking type [36].

We found positive values for the enthalpy of activation,  $37.6 \text{ kJ mol}^{-1}$  for the blank and  $39.9 \text{ kJ mol}^{-1}$  for Inhibitor 1, demonstrating the endothermic nature of the mild steel dissolution. The calculated enthalpies were lower than the activation energies, suggesting that the corrosion process occurs through a gaseous reaction, and this may be due to the hydrogen evolution associated with a decrease in the total volume of the reaction. The difference  $E_a - \Delta H$  is equal to  $RT$  ( $2.6 \text{ kJ mol}^{-1}$ ), a clue that the metal dissolution is a unimolecular reaction [36, 37].

The analysis of the entropy of activation showed that assays containing the extract ( $-114 \text{ J K}^{-1} \text{ mol}^{-1}$ ) and the blank ( $-111 \text{ J K}^{-1} \text{ mol}^{-1}$ ) have very similar results. This suggests that the adsorption of the extract molecules is a quasi-substitution process, which means that the adsorption of the inhibitor molecules is accompanied by desorption of water molecules. The thermodynamic values are the algebraic sum between the adsorption of the inhibitor and the desorption of water molecules [38, 39].

### 3.1.2. Electrochemical measurements

#### 3.1.2.1. Potentiodynamic polarization measurements

Fig. 2 shows that inhibitor 1 displaced both anodic and cathodic branches of the curves for all tested concentrations. Although the decrease in current densities was more pronounced for the cathodic section, the dislocation of the  $E_{\text{corr}}$  was less than  $85 \text{ mV}$ , so inhibitor 1 could be characterized as a mixed type inhibitor [9].

It is interesting to note that the  $OCP$  values showed a small anodic displacement with respect to the blank, whereas the  $E_{\text{corr}}$  showed a cathodic shift. These results suggest that under  $OCP$  the inhibitor

slowed down both anodic and cathodic reactions, acting as a mixed type inhibitor with a slight anodic character. However, when the mild steel is polarized, this behavior changes, shifting the  $E_{corr}$  to more negative values, showing that the inhibitory molecule adsorption depends on the applied potential.

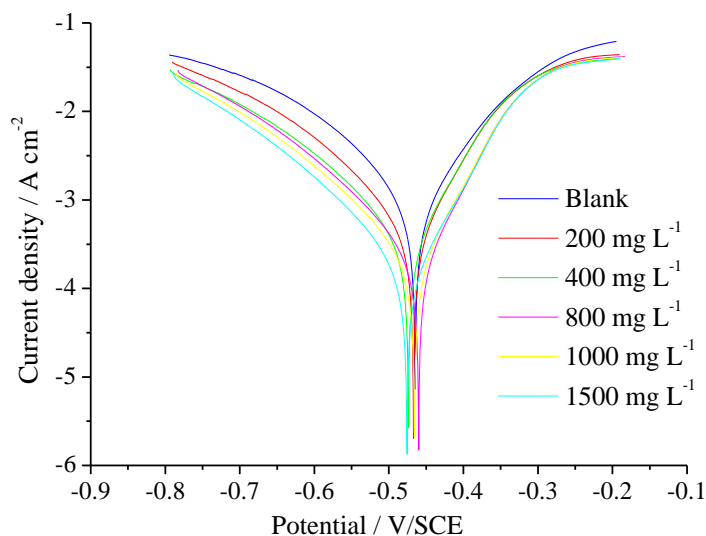


**Figure 2.** Polarization curves for mild steel in 1 mol L<sup>-1</sup> HCl in the absence and presence of different concentrations of inhibitor 1.

Electrochemical parameters (Table 3) reinforces the observations made in Fig. 2.  $j_{corr}$  values decreased as the extract concentration increased, suggesting the formation of a protective layer on the metal surface. The Tafel constant  $\beta_c$  did not significantly vary with inhibitor 1 addition, suggesting that the real area available for H<sup>+</sup> ions diminishes as the inhibitor adsorbs, so the reduction mechanism remains the same, but the active area is smaller, reflected in the displacement of the cathodic sector of the polarization curves [8, 5, 40].

**Table 3.** Electrochemical parameters obtained from polarization curves for inhibitor 1.

Concentration (mg L <sup>-1</sup> )	OCP (mV)	$E_{corr}$ (mV)	$j_{corr}$ (mA cm <sup>-2</sup> )	$\beta_a$ (mV dec <sup>-1</sup> )	$-\beta_c$ (mV dec <sup>-1</sup> )	IE (%)
0	-496	-446	1.12	91.6	173	-
200	-491	-450	0.517	69.8	155	53.9
400	-494	-457	0.428	70.2	162	61.9
800	-484	-446	0.227	60.8	140	79.8
1000	-485	-454	0.207	64.5	137	81.6
1500	-489	-458	0.182	66.0	143	83.8

### 3.1.2.2. Electrochemical impedance spectroscopy (EIS)

We observed only one capacitive loop (Fig. 3) for both uninhibited and inhibited assays, which could be attributed to the charge transfer and double layer capacitance. This indicates that the

corrosion mechanism remained the same for all the studied cases, regardless of the presence of the extracts. Moreover, the diameter of the loop increased with increasing inhibitor concentrations and showed a depressed shape. We could attribute this behavior to the inhomogeneity of the surface due to the corrosion process. This is also the reason why we used a constant phase element (CPE) instead of a double layer capacitor in the data analysis.

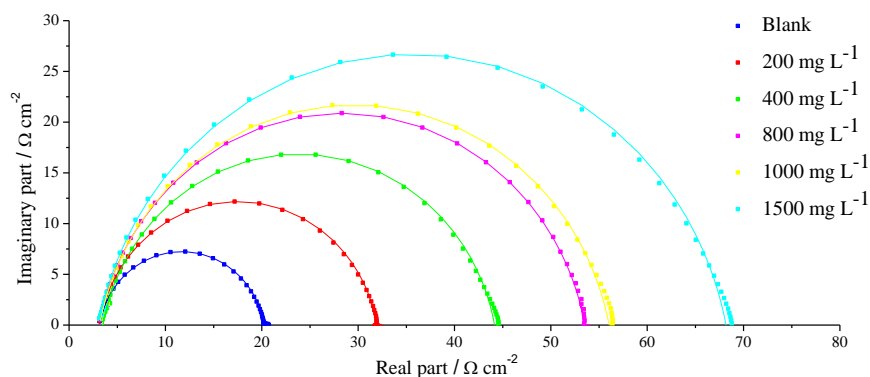


**Figure 3.** Electrochemical impedance diagrams for mild steel in 1 mol L<sup>-1</sup> HCl medium in the presence and absence of different concentrations of inhibitor 1.

We analyzed all the diagrams obtained based on an equivalent circuit shown in Fig. 4.  $R_s$  is the solution resistance,  $R_{ct}$  is the charge transfer resistance, and  $CPE$  is the constant phase element.

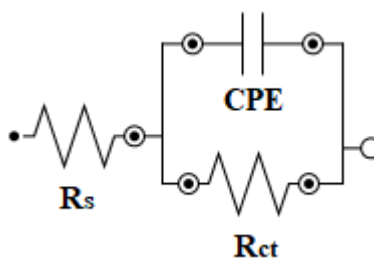


**Figure 4.** Equivalent circuit used for impedance simulations.

The  $CPE$  was calculated using equation 7, as follows [41]:

$$Z_{CPE} = 1/Y_0(j\omega)^n \tag{7}$$

Where  $Y_0$  is the magnitude of  $CPE$  and  $n$  represents the deviation from the ideal behavior falling between -1 and 1.

We calculated the double layer capacitance,  $C_{dl}$ , for the  $CPE$  including circuit based on equation 8, as follows [41]:

$$C_{dl} = Y_0(\omega_{max})^{n-1} \tag{8}$$

Where  $\omega_{max} = 2\pi f_{max}$ , and  $f_{max}$  is the frequency in which the imaginary component of the impedance is maximal.

The  $C_{dl}$  values decreased while  $R_{ct}$  increased as the inhibitor concentration increased. The  $f_{max}$  remains constant with inhibitor addition (Table 4). All these results agree with the hypothesis that inhibitor 1 could be a purely blocking type inhibitor by only reducing the active area of the electrode.

**Table 4.** Electrochemical parameters obtained from the electrochemical impedance spectroscopy for inhibitor 1.

Concentration (mg L <sup>-1</sup> )	$f_{max}$ (Hz)	$C_{dl}$ ( $\mu\text{F cm}^{-2}$ )	$R_{ct}$ ( $\Omega \text{ cm}^2$ )	$n$	$IE$ (%)
0	56.7	158	17.2	0.889	-
200	56.7	100	28.8	0.887	40.3
400	56.7	77.3	41.1	0.864	58.1
800	35.5	73.2	50.4	0.875	65.9
1000	56.7	59.0	53.1	0.869	67.7
1500	44.9	59.5	65.4	0.877	73.7

From the calculated degree of surface coverage, it was possible to study different adsorption isotherms. Langmuir Isotherm (Eq. 9) presented the best correlation coefficient in order to ascertain the adsorption characteristics of the extract, shown in Fig. 5.

$$C/\theta = 1/K_{ads} + C \tag{9}$$

The correlation coefficient obtained for the straight line was 0.9987 with an angular coefficient of 1.2057, suggesting the formation of a protective monolayer on the metal surface with a fixed number of adsorption sites. The angular coefficient is higher than 1. This deviation of Langmuir behavior suggests that the adsorbed molecules can occupy more than one active site [30, 42].

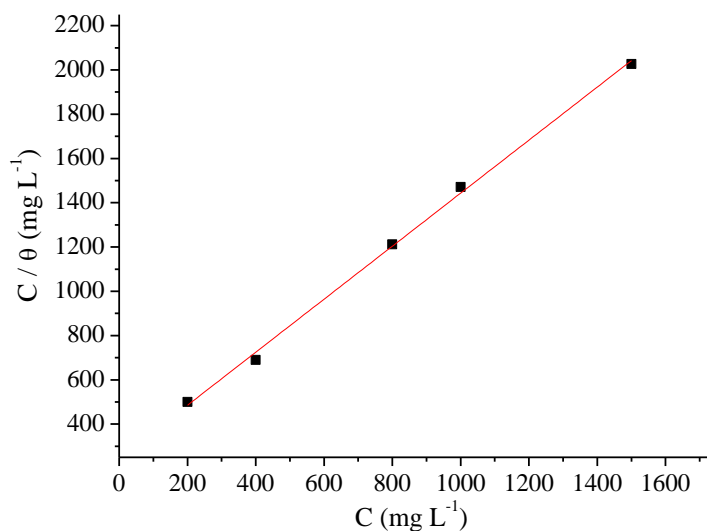


**Figure 5.** Langmuir isotherm for the adsorption of inhibitor 1 onto mild steel surface.

### 3.2. Study of the High Molecular Weight Fraction (HMWF) obtained from the aqueous coffee husk extract – Inhibitor 2

There is no consensus on which group of substances present in coffee husks are responsible for the inhibitory effect. Our group tested low molecular phenolic compounds such as chlorogenic acids and alkaloids [29, 30], but they did not seem to be responsible for corrosion inhibition. Then, we isolated the HMWF from roasted coffee extract [30] and accomplished interesting results. Some researches stated that coffee HMWF [43, 44] showed the presence of molecules containing heteroatoms with high electron density, such as nitrogen and oxygen, or molecules with multiple bonds. Based on these studies, we decided to isolate the HMWF (heavier than 3 kDa) from coffee husks and test it as a corrosion inhibitor.

#### 3.2.1. Gravimetric measurements

Inhibitor 2 seems to be more dependent on the time than on the concentration. In short immersion times, it showed dependence on concentration, in higher immersion time the concentration did not seem to affect significantly.  $W_{corr}$  decreased with increasing time, leading to higher  $IE$  (Table 5). This is a sign that a protective and stable layer was formed upon the metal surface even in lower concentration of the extract. We tested a lower concentration (50 mg L<sup>-1</sup>) and observed it was possible to obtain high  $IE$  with lower extract quantity.

**Table 5.** Results of the gravimetric assays for mild steel varying time and concentration of inhibitor 2.

Immersion time (h)	Inhibitor (mg L <sup>-1</sup> )	$W_{corr}$ (g cm <sup>-2</sup> h <sup>-1</sup> )	Standard deviation (g cm <sup>-2</sup> h <sup>-1</sup> )	$IE$ (%)
2	0	3.04 x 10 <sup>-3</sup>	5 x 10 <sup>-5</sup>	-
	50	1.55 x 10 <sup>-3</sup>	2 x 10 <sup>-5</sup>	48.9
	100	1.23 x 10 <sup>-3</sup>	3 x 10 <sup>-5</sup>	59.6
	400	1.07 x 10 <sup>-3</sup>	3 x 10 <sup>-5</sup>	64.7
	800	1.22 x 10 <sup>-3</sup>	2 x 10 <sup>-5</sup>	64.1
24	0	1.95 x 10 <sup>-3</sup>	2 x 10 <sup>-5</sup>	-
	50	2.35 x 10 <sup>-4</sup>	7 x 10 <sup>-6</sup>	88.0
	100	2.12 x 10 <sup>-4</sup>	1 x 10 <sup>-5</sup>	89.1
	400	1.64 x 10 <sup>-4</sup>	8 x 10 <sup>-6</sup>	91.6
	800	1.93 x 10 <sup>-4</sup>	3 x 10 <sup>-6</sup>	90.3

For all inhibitors concentrations, the HMWF presented higher *IE* than the coffee husk extract. This could be associated with an extract enrichment by the molecules responsible for the protective effect or by the nature of the adsorbed molecules.

We also carried out tests varying temperature using 200 mg L<sup>-1</sup> of inhibitor 2 for 2 h to analyze the effects of heating the system (Table 6).

**Table 6.** Results of the gravimetric tests in the presence and absence of 200 mg L<sup>-1</sup> of inhibitor 2 for 2 hours varying temperature.

Temperature (°C)	Blank		Inhibitor 2		<i>IE</i> (%)
	<i>W<sub>corr</sub></i> (g cm <sup>-2</sup> h <sup>-1</sup> )	Standard deviation (g cm <sup>-2</sup> h <sup>-1</sup> )	<i>W<sub>corr</sub></i> (g cm <sup>-2</sup> h <sup>-1</sup> )	Standard deviation (g cm <sup>-2</sup> h <sup>-1</sup> )	
25	3.00 x 10 <sup>-3</sup>	1 x 10 <sup>-4</sup>	1.22 x 10 <sup>-3</sup>	1 x 10 <sup>-5</sup>	59.2
35	4.62 x 10 <sup>-3</sup>	<1 x 10 <sup>-5</sup>	1.48 x 10 <sup>-3</sup>	<1 x 10 <sup>-5</sup>	67.9
45	8.62 x 10 <sup>-3</sup>	5 x 10 <sup>-5</sup>	1.98 x 10 <sup>-3</sup>	9 x 10 <sup>-5</sup>	77.0
55	1.21 x 10 <sup>-3</sup>	<1 x 10 <sup>-3</sup>	3.14 x 10 <sup>-3</sup>	2 x 10 <sup>-4</sup>	74.0

There was an increase in the *IE* with the temperature, from 59.2% to 77.0%. This result indicates that the adsorption of the molecules present in the extract 2 was favored and became more effective as the temperature increased [35], thereby slowing the corrosion process [14].

The activation parameters for mild steel corrosion in the presence of inhibitor 2 were calculated using equations 2 and 6 and the Arrhenius plots (Fig. 6). The *E<sub>a</sub>* was 40.2 kJ mol<sup>-1</sup> in the absence and 26.4 kJ mol<sup>-1</sup> in the presence of Inhibitor 2. The  $\Delta H^*$  values were 37.6 kJ mol<sup>-1</sup> in the absence and 23.9 kJ mol<sup>-1</sup> in the presence of the inhibitor. The decrease of these values can be related to a chemisorption process [40, 45], associated to a charge transfer from the inhibitor molecules to the mild steel surface. This hypothesis is confirmed by the increase in the *IE* with increasing temperature [35]. The values of  $\Delta S^*$  in the absence (-111 J K<sup>-1</sup> mol<sup>-1</sup>) and presence (-57.3 J K<sup>-1</sup> mol<sup>-1</sup>) of the inhibitor are negative, a sign that the activated complex in the rate determining step is related to an association instead of a dissociation step [37].

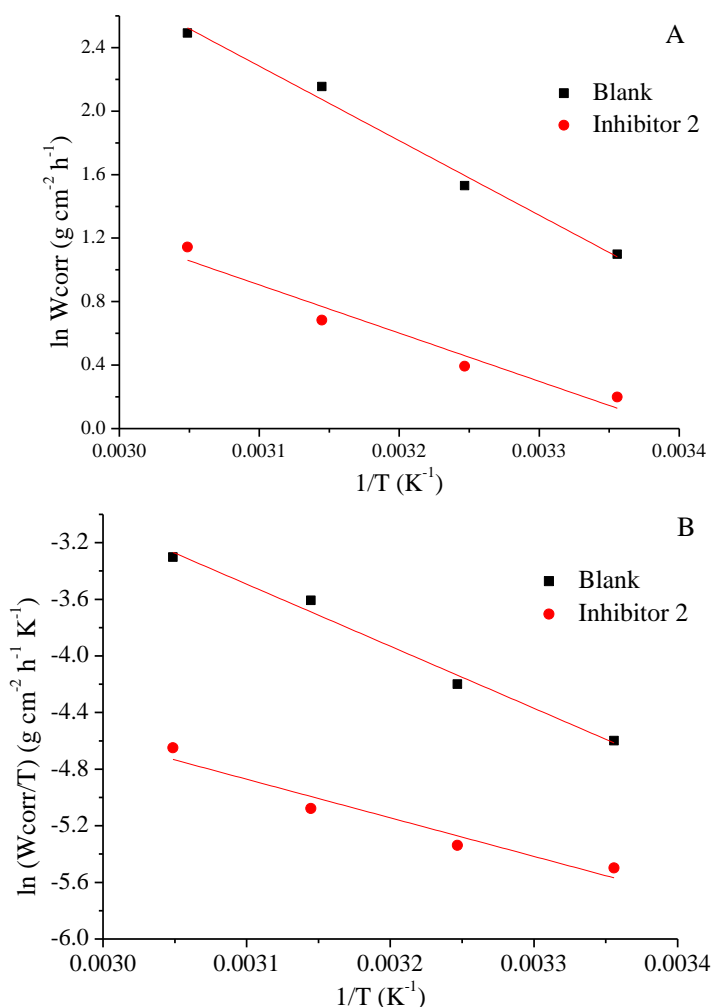


**Figure 6.** Arrhenius plot (A)  $\ln W_{corr} \times 1/T$  and (B)  $\ln(W_{corr}/T) \times 1/T$  for mild steel in 1 mol L<sup>-1</sup> in the absence and presence of inhibitor 2.

Inhibitor 2 affects the corrosion activation energy and screens the metal surface, like the majority of organic inhibitors [36]. This behavior is contrary to expectations, since in our work with coffee grounds [30], its HMWF presented the same demeanor as the aqueous extract with the temperature variation. In present study the HMWF presented better performance for all the tested conditions, which may be due to the nature of the macromolecules that adhere to the metal surface in a more effective way.

### 3.2.2. Electrochemical measurements

#### 3.2.2.1. Potentiodynamic polarization measurements

Lower concentrations were used for inhibitor 2 in comparison with inhibitor 1. Similar tendencies were observed, but inhibitor 2 showed a better performance. *OCP* values remained almost constant (Table 7), suggesting a mixed type inhibitor.  $j_{corr}$  decreased as the extract concentration

increased, leading to higher  $IE$  and indicating the suppression of the corrosion process. The change in  $E_{corr}$  to more negative values shows the dependence of the adsorption process on the applied potential, being more effective at cathodic polarization, as was seen for the inhibitor 1 (Fig. 7).

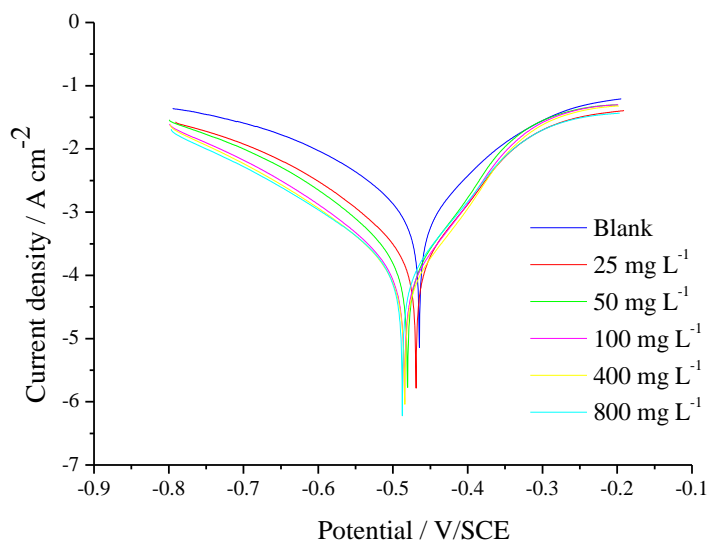


**Figure 7.** Polarization curves for mild steel in 1 mol L<sup>-1</sup> HCl in the absence and presence of different concentrations of inhibitor 2.

**Table 7.** Electrochemical parameters obtained from polarization curves for inhibitor 2.

Concentration (mg L <sup>-1</sup> )	OCP (mV)	$E_{corr}$ (mV)	$j_{corr}$ (mA cm <sup>-2</sup> )	$\beta_a$ (mV dec <sup>-1</sup> )	$-\beta_c$ (mV dec <sup>-1</sup> )	$IE$ (%)
0	-495	-446	1.12	91.6	173	-
25	-491	-453	0.210	65.1	128	81.3
50	-499	-461	0.165	59.9	126	85.3
100	-499	-467	0.114	61.0	128	89.8
400	-498	-463	0.110	61.0	135	90.2
800	-497	-472	0.130	67.8	140	88.4

For a given immersion time the  $IE$  is almost steady from 100 mg L<sup>-1</sup> onward; this may be due to a saturation of the metal surface with the molecules responsible for the corrosion inhibition, achieving an efficiency of 90.2% for a concentration of 400 mg L<sup>-1</sup>.

### 3.2.2.2. Electrochemical impedance spectroscopy (EIS)

Once again, the HMWF presented the same tendencies detected for coffee husk extract, Fig. 8 shows the same behavior for the uninhibited and inhibited assays. The capacitive loop presented for

uninhibited and inhibited system is related to the charge transfer and double-layer capacitance. The diameter of the loops increased with increasing extract concentration and showed a depressed shape, which can be attributed to metallic surface inhomogeneity due to the corrosion process [34]. These results were consistent with the ones obtained from the polarization curves, confirming the inhibitor adsorption onto the mild steel surface.

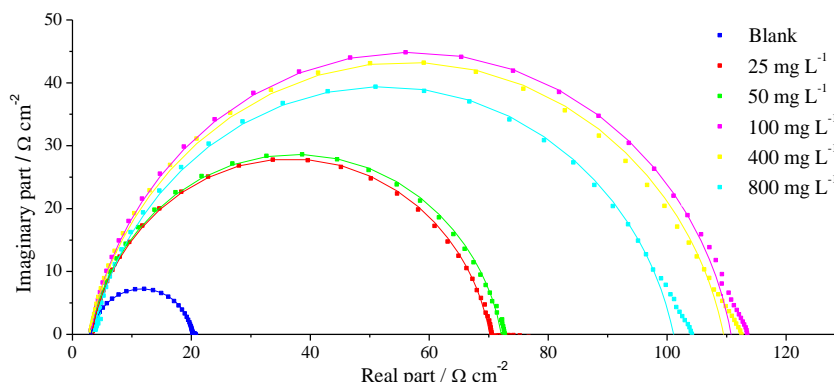


**Figure 8.** Electrochemical impedance diagrams for mild steel in 1 mol L<sup>-1</sup> HCl medium in the presence and absence of different concentrations of inhibitor 2.

We used the equivalent circuit of Fig. 4 to analyze the diagrams as done for inhibitor 1. Table 8 shows the data obtained from the diagrams and calculated using the equivalent circuit.

**Table 8.** Electrochemical parameters obtained from the electrochemical impedance spectroscopy for inhibitor 2.

Concentration (mg L <sup>-1</sup> )	$f_{max}$ (Hz)	$C_{dl}$ ( $\mu\text{F cm}^{-2}$ )	$R_{ct}$ ( $\Omega \text{ cm}^2$ )	$n$	$IE$ (%)
0	56.7	158	17.2	0.889	-
25	35.5	75.5	67.7	0.889	74.6
50	35.5	63.5	69.6	0.887	75.3
100	28.1	54.4	109	0.882	84.2
400	28.1	50.5	108	0.879	84.1
800	35.5	48.3	98.9	0.871	82.6

The increasing addition of inhibitor 2 in acidic media decreased the  $C_{dl}$  and increased the  $R_{ct}$  due to a lower available area for corrosion process. The HMWF behaved similarly to the aqueous coffee husk extract by blocking the metal surface. The  $f_{max}$  has decreased somewhat with the addition of inhibitor 2, which may be caused by a reduction in the local dielectric constant and/or by an increase in the thickness of the electrical double layer [18, 20]. The degree of coverage increases but seems to remain almost constant from 100 mg L<sup>-1</sup>, probably due to the metal surface saturation, which was

reflected in the  $IE$  that is nearly constant by 84%. Fig. 9 shows the Langmuir's plot for the HMWF extract [20].

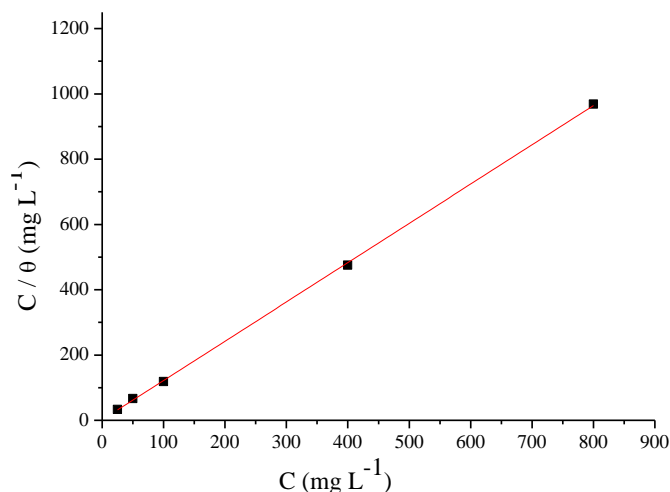


**Figure 9.** Langmuir isotherm for the adsorption of inhibitor 2 onto mild steel surface.

The correlation coefficient obtained for the straight line was 0.9997 and the angular coefficient was 1.2038, which is consistent with the formation of a protective monolayer. As it was verified for inhibitor 1, the angular coefficient was also higher than 1, indicating that the adsorbed molecules were big enough to cover more than one active site.

We observed slight differences between the gravimetric and electrochemical  $IE$  results. This may be due to the difference in the surface treatment [19] and to the exposure time of the experiments. However, the results are in good agreement with each other, reinforcing the formation of a protective layer onto the mild steel working electrode.

### 3.3. Surface morphological examination

#### 3.3.1. Scanning Electron Microscopy (SEM)

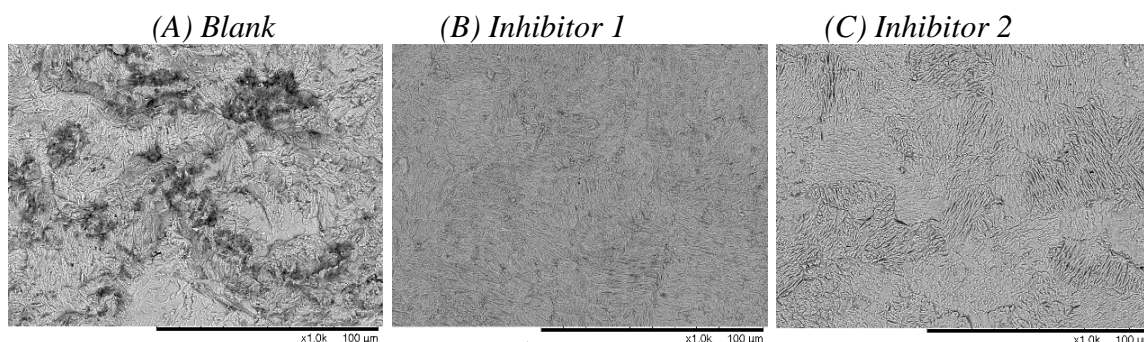


**Figure 10.** SEM photographs of mild steel surface after 24h of immersion period: (A) 1.0 M HCl, (B) 1.0 M HCl + 200 mg L<sup>-1</sup> Inhibitor 1, (C) 1.0 M HCl + 200 mg L<sup>-1</sup> Inhibitor 2.

The morphology observed in Fig. 10A is that of a rough surface, characteristic of a uniform acid corrosion process in which the unprotected metal surface was highly damaged. On the other hand, a smoother surface was observed in Figs. 10B and C, where extracts 1 and 2 were present, indicating that the surface was protected by the extracts, which corroborates with the previously discussed electrochemical assays.

The mild steel can be effectively protected against acid corrosion by natural products. There are some examples from the literature of extracts obtained from natural sources that achieved high inhibition efficiencies [17, 29, 40, 46]. Table 9 shows the highest *IE* obtained for the cited inhibitors by weight loss measurements. All cited inhibitors act as mixed type, suppressing both the anodic and cathodic reactions in the polarization curves. It is important to emphasize that coffee husks are the major solid residues from coffee processing. The high inhibition efficiency of its extract is clearly an opportunity for adding value to this kind of residue, which has been treated as a waste by the industry.

**Table 9.** Different natural corrosion inhibition for mild steel in HCl media.

Inhibitor	Concentration (mg L <sup>-1</sup> )	Inhibitor type	Inhibition efficiency (%)	Ref
Gum Arabic Acacia	1000	Mixed type	95	46
Papaya seed extract	400	Mixed type	94	17
Pomegranate leaves extract	1000	Mixed type	94	40
Coffee grounds extract	400	Mixed type	97	29
Coffee husks extract	1000	Mixed type	94	Present work
HMWF of coffee husks extract	400	Mixed type	92	Present work

#### 3.4. Spectroscopic characterization by nuclear magnetic resonance (NMR)

Both spectra (Fig. 11 A and B) show similar signals: methyl and aliphatic hydrogens of proteins (from 1.0 to 1.5 ppm), aliphatic hydrogens of organic acids or their esters (from 1.5 to 3.0 ppm), hydroxylic hydrogens of polysaccharides (highly overlapped resonance signals from 3.0 to 5.0 ppm), anomeric hydrogens of polysaccharides (from 5.0 to 5.5 ppm), and aromatic and olefinic hydrogens from chlorogenic acids, caffeine or trigonelline (from 6.0 to 9.5 ppm) [47, 48].

These results indicate that both extracts contained macromolecules, such as proteins and polysaccharides, mainly hemicellulose [49], in addition to small molecules, such as organic acids, chlorogenic acids, caffeine and trigonelline. These small molecules were still present in inhibitor 2, probably because they were not completely removed from the aqueous coffee husk extract (inhibitor 1) during diafiltration. The spectra are within the expected, according to previously published literature data, and mainly presented signals related to the presence of polysaccharides and proteins [47, 49], with extract 2 enriched with macromolecules due to diafiltration.

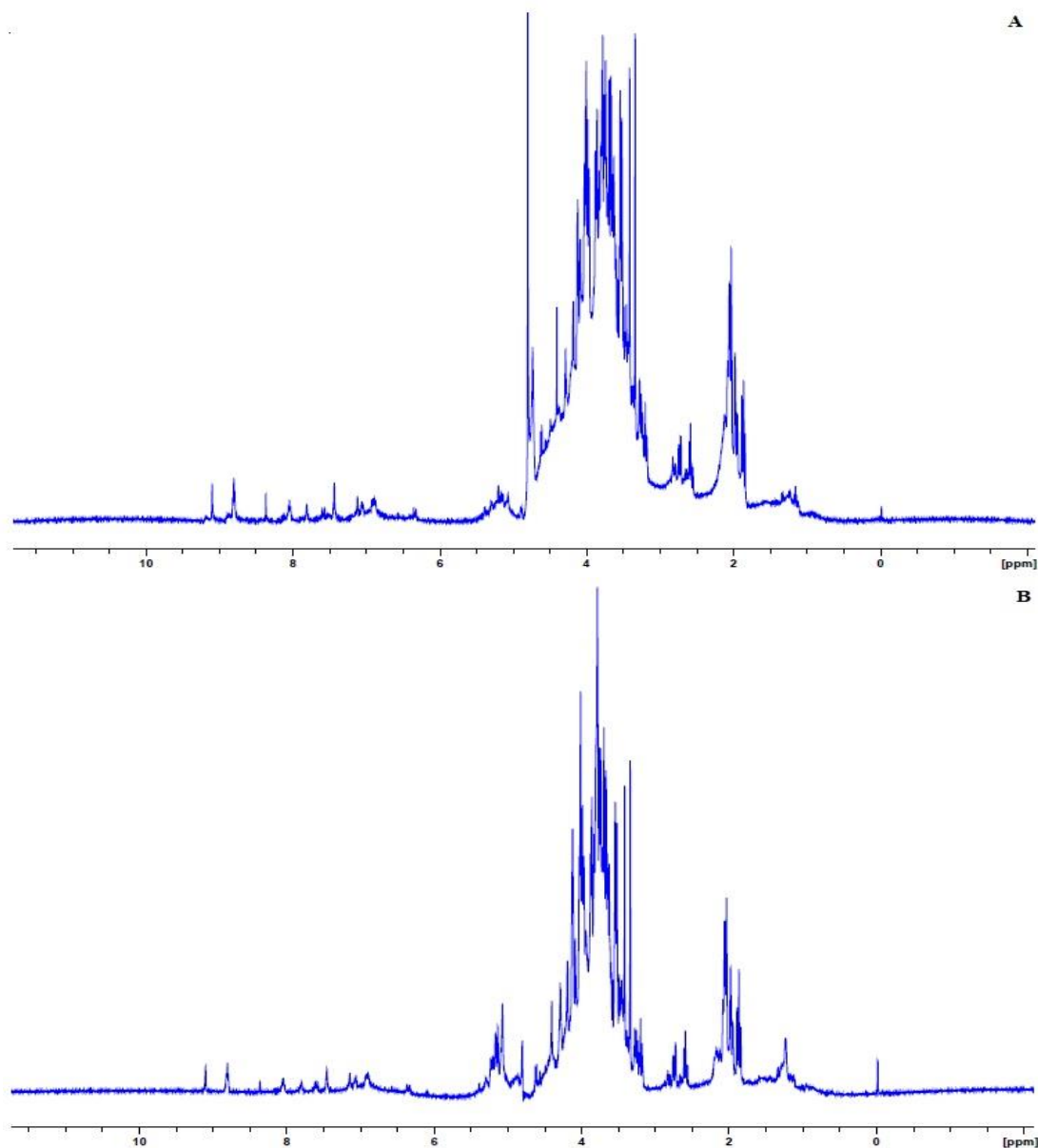


**Figure 11.**  $^1\text{H}$  NMR spectra of inhibitors 1 (A) and 2 (B).

#### 4. CONCLUSIONS

- Both extracts (coffee husk aqueous extract and its HMWF) act as good corrosion inhibitors for mild steel in acidic media;
- The adsorption process takes up to 24 hours to saturate the electrode surface with the inhibitor molecules;
- Inhibitor 1 seems to act just by blocking the mild steel surface, not changing the activation energy for the corrosion process of the metal in acidic media. Whereas its HMWF acted as the majority of organic corrosion inhibitors, changing the activation energy and blocking the metal surface;

- As the inhibition efficiency did not decrease with the increase of the temperature for both inhibitors, it can be inferred there is a chemisorption process;
- Both inhibitors act as mixed type, decreasing both cathodic and anodic current densities;
- Impedance diagrams obtained for both inhibitors were very similar, indicating they block the metal surface, decreasing the active area, reflecting in an increase of polarization resistance and decrease in the double layer capacitance;
- SEM images corroborated with the gravimetric and electrochemical results and showed that mild steel surface is much less corroded when in the presence of inhibitors 1 and 2;
- NMR analysis showed both extracts contained macromolecules, such as proteins and polysaccharides and small molecules such as organic acids, chlorogenic acids, caffeine and trigonelline. Despite their similar compositions, diafiltration led to the concentration of macromolecules present in HMWF;
- The HMWF presented higher *IE* compared to the aqueous husk extract; however, they acted under different mechanisms. Inhibitor 1 acted only by blocking the metal surface while Inhibitor 2 acted by blocking the surface and decreased the activation energy. Therefore, the highest *IE* observed for inhibitor 2 cannot be inferred solely to the increase on the macromolecules concentration in HMWF.

#### ACKNOWLEDGEMENTS

This work was supported by CNPq (National Council for Scientific and Technological Development) (153940/2015-8, 424306/2016 and 309353/2015-7) and by FAPERJ (Fundação de Amparo à Pesquisa do Estado do Rio de Janeiro) (E-26/010.001675/2014).

#### References

1. S.S.A.A. Pereira, M.Sc. Dissertation, *IQ/UFRJ* (2009) 1.
2. A.A. Silva, M.Sc. Dissertation, *IQ/UEP* (2009) 1.
3. E.E. Oguzie, *Corros. Sci.*, 50 (2008) 2993.
4. H. Bentrach, Y. Rahali and A. Chala, *Corros. Sci.*, 82 (2014) 426.
5. A.Y. El-Etre and M. Abdallah, *Corros. Sci.*, 42 (2000) 731.
6. O.K. Abiola and J.O.E. Otaigbe, *Corros. Sci.*, 51 (2009) 2790.
7. M. Mobin and M. Rizvi, *Carbohydr. Polym.*, 160 (2017) 172.
8. M. Abdallah, *Portug. Electroch. Acta*, 22 (2004) 161.
9. M.M. Fares, A.K. Maayta and J.A. Al-Mustafa, *Corros. Sci.*, 65 (2012) 223.
10. M. Fiori-Bimbia, A. Victoria, E. Patricia, H. Vacca and C.A. Gervasic, *Corros. Sci.*, 92 (2014) 192.
11. P. Mourya, S. Banerjee and M.M. Singh, *Corros. Sci.*, 85 (2014) 352.
12. P.B. Raja and M.G. Sethuraman, *Mater. Lett.*, 62 (2008) 113.
13. A. Bouyanzer, B. Hammouti and L. Majidi, *Mater. Lett.*, 60 (2006) 2840.
14. R.S. Trindade, M.R. Santos, R.F.B. Cordeiro and E. D'Elia, *Green Chem. Lett. Rev.*, 10 (2017) 444.
15. L.A.C. Matos, P.R.P. Rodrigues, E. D'Elia, N. Boschen, G.A.R. Maia and M.T. Cunha, *Rev. Prop. Ind.*, 1 (2017) 313.

16. K. Ribeiro, R.F.B. Cordeiro, H. Orofino, J.C. Nunes, M. Magalhães, A. G. Torres and E. D'Elia, *Int. J. Electrochem. Sci.*, 11 (2016) 406.
17. V.V. Torres, G.B.Cabral, A.C.G. Silva, K.C.R. Ferreira and E. D'Elia, *Quim. Nova*, 39 (2016) 423.
18. J.C. Rocha, J.A.C.P. Gomes and E. D'Elia, *Mater. Res.*, 17 (2014) 1581.
19. S.S. Assunção, M.M. Pêgas, T.L. Fernandez, M. Magalhães, T.G. Schöntag, D.C.B. Lago and E. D'Elia, *Corros. Sci.*, 65 (2012) 360.
20. J.C. Rocha, J.A.P. Gomes, J.A. Cunha and E. D'Elia, *Corros. Sci.*, 52 (2010) 2341.
21. A.R.P. Parra, I. Moreira, A.C. Furlan, D. Paiano, C. Scherer and P.L.O. Carvalho, *R. Bras. Zootec.*, 37 (2008) 433.
22. F.S. Souza, R.S. Gonçalves and A. Spinelli, *J. Braz. Chem. Soc.*, 25 (2014) 81.
23. A.R. Lima, R.G.F.A. Pereira, S.A. Abrahão, S.M.S. Duarte and F.B.A. Paula, *Quim. Nova*, 33 (2010) 20.
24. Y. Narita and K. Inouye, *Food Res. Int.*, 61 (2014) 16.
25. L. Bresciani, L. Calani, R. Bruni, F. Brighenti and D.D. Rio, *Food Res. Int.*, 61 (2014) 196.
26. P. Esquivel and V.M. Jiménez, *Food Res. Int.*, 46 (2012) 488.
27. D. Perrone, D.Sc. dissertation, IQ/UFRJ (2009) 1.
28. Conab, *Obs. Agr.*, (2017) 1.
29. V.V. Torres, R.S. Amado, C.F. Sa, T.L. Fernandez, C.A.S. Riehl, A.G. Torres and E. D'Elia, *Corros. Sci.*, 53 (2011) 2385.
30. E.C.C.A. Souza, B.A. Ripper, D. Perrone and E. D'Elia, *Mater. Res.*, 19 (2016) 1276.
31. E.K. Bekedem, H.A. Schols, M.A.J.S. Van Boekel and G. Smit, *J. Agric. Food Chem.*, 54 (2006) 7658.
32. F.M. Nunes and M.A. Coimbra, *J. Agric. Food Chem.*, 55 (2007) 3967.
33. R.C. Borelli, A. Visconti, C. Mennella, M. Anese and V. Fogliano, *J. Agric. Food Chem.*, 50 (2002) 6527.
34. F.S. Souza and A. Spinelli, *Corros. Sci.*, 51 (2009) 642.
35. C.O. Akalezi, C.E. Ogukwe, E.A. Ejele and E.E. Oguzie, *Int. J. Corros. Scale Inhib.*, 5 (2016) 132.
36. Y.I. Kuznetsov, N.N. Andreev and S.S. Vesely, *Int. J. Scale Inhb.*, 4 (2015) 08.
37. Q. Zhang and Y. Hua, *Mater. Chem. Phys.*, 119 (2010) 57.
38. B.G. Ateya, B.E. El-Anadauli and F.M. El-Nizamy, *Corros. Sci.*, 24 (1984) 509.
39. X.H. Li, S.D. Deng, G.N. Mu, H. Fu and F.Z. Yang, *Corros. Sci.*, 50 (2008) 420.
40. Y. Abboud, O. Tanane, A. El Bouari, R. Salghi, B. Hammouti, A. Chetouani and S. Jodeh, *Corros. Eng. Sci. and Tech.*, 51 (2016) 557.
41. S.K. Singh, S.P. Tambe, G. Gunasekaran, V.S. Raja and D. Kumar, *Corros. Sci.*, 51 (2009) 595.
42. S.J. Olusegum, T.S. Joshua, M.O. Bodunrin and S. Aribo, *Nat. and Sci.*, 16 (2018) 1.
43. M. Daglia, A. Papetti, C. Aceti, B. Sordelli, C. Gregotti and G. Gazzani, *J. Agric. Food Chem.*, 56 (2008) 11653.
44. J. Bravo, C. Monente, I. Juániz, P. De Peña and C. Cid, *Food Res. Int.*, 50 (2013) 610.
45. I. Ahamad, R. Prasad and M.A. Quraishi, *J. Solid State Electrochem.*, 14 (2010) 2095.
46. K. Azzaoui, E. Mejdoubi, S. Jodeh, A. Lamhamdi, E. R. Castellón, M. Algarra, A. Zarrouk, A. Errich, R. Salghi and H. Lgaz, *Corros. Sci.*, 129 (2017) 70.
47. F.W. Furihata, K.F. Hu, T. Miyakawa and M. Tanokura, *J. Agric. Food Chem.*, 59 (2011) 9065.
48. M. Bosco, R. Toffanin, D. Palo, L. Zatti and A. Segre, *J. Sci. Food Agric.*, 79 (1999) 869.
49. S.A. Bekalo and R. Hans-Wolf, *Mat. and Struct.*, 43 (2010) 1049.